CLINICS

CLINICAL SCIENCE

The development and evaluation of individualized templates to assist transoral C2 articular mass or transpedicular screw placement in TARP-IV procedures: adult cadaver specimen study

Xue-Shi Li,[I,II] Zeng-Hui Wu,[I*] Hong Xia,[I] Xiang-Yang Ma,[I] Fu-Zhi Ai,[I] Kai Zhang,[I] Jian-Hua Wang,[I] Xiao-Hong Mai,[I] Qing-Shui Yin[I*]

[I]Guangzhou General Hospital of Guangzhou Military Command (Liuhuaqiao Hospital), Institute of Traumatic Orthopaedics of People's Liberation Army, Key Laboratory of Orthopaedic Tecnology and Implant Materials of Guangdong Province, Department of Orthopedics, Guangzhou, 510010, People's Republic of China. [II]Southern Medical University, Guangzhou, 510515, People's Republic of China.

OBJECTIVES: The transoral atlantoaxial reduction plate system treats irreducible atlantoaxial dislocation from transoral atlantoaxial reduction plate-I to transoral atlantoaxial reduction plate-III. However, this system has demonstrated problems associated with screw loosening, atlantoaxial fixation and concealed or manifest neurovascular injuries. This study sought to design a set of individualized templates to improve the accuracy of anterior C2 screw placement in the transoral atlantoaxial reduction plate-IV procedure.

METHODS: A set of individualized templates was designed according to thin-slice computed tomography data obtained from 10 human cadavers. The templates contained cubic modules and drill guides to facilitate transoral atlantoaxial reduction plate positioning and anterior C2 screw placement. We performed 2 stages of cadaveric experiments with 2 cadavers in stage one and 8 in stage two. Finally, guided C2 screw placement was evaluated by reading postoperative computed tomography images and comparing the planned and inserted screw trajectories.

RESULTS: There were two cortical breaching screws in stage one and three in stage two, but only the cortical breaching screws in stage one were ranked critical. In stage two, the planned entry points and the transverse angles of the anterior C2 screws could be simulated, whereas the declination angles could not be simulated due to intraoperative blockage of the drill bit and screwdriver by the upper teeth.

CONCLUSIONS: It was feasible to use individualized templates to guide transoral C2 screw placement. Thus, these drill templates combined with transoral atlantoaxial reduction plate-IV, may improve the accuracy of transoral C2 screw placement and reduce related neurovascular complications.

KEYWORDS: Transoral Atlantoaxial Reduction Plate; Accuracy; Atlantoaxial Dislocation; Transoral Transpedicular Screw.

Li XS, Wu ZH, Xia H, Ma XY, Ai FZ, Zhang K, et al. The development and evaluation of individualized templates to assist transoral C2 articular mass or transpedicular screw placement in TARP-IV procedures: adult cadaver specimen study. Clinics. 2014;69(11):750-757.

Received for publication on May 19, 2014; **First review completed on** July 2, 2014; **Accepted for publication on** August 25, 2014

E-mail: wzh2899@163.com (Zeng-Hui Wu)/gz_yqs@126.com (Qing-Shui Yin)

*co-corresponding authors

Tel.: 86-20-36653539

INTRODUCTION

The surgical treatment of irreducible atlantoaxial dislocation (IAAD) is a challenge for neurospinal surgeons and a variety of procedures have been developed with varying levels of success (1-4). Among them, anterior transoral release followed by posterior atlantoaxial screw and plate/rod instrumentation is considered the benchmark procedure. However, the need to turn the patient over intraoperatively after atlantoaxial release, a prolonged operative time and additional posterior iatrogenic trauma make this a less favorable and potentially risky procedure. We therefore developed the transoral atlantoaxial reduction plate (TARP) system, with which transoral release, reduction, internal fixation and bone grafting can be achieved in a one-stage operation (4). During clinical application, we improved this approach from TARP-I to TARP-III, in which the C2 transoral articular mass screw or the C2 transoral transpedicular screw (C2TOAMS/C2TOTPS) (Figure 1) was adopted (5). Although this screw is sufficiently rigid to

No potential conflict of interest was reported.

DOI: 10.6061/clinics/2014(11)08

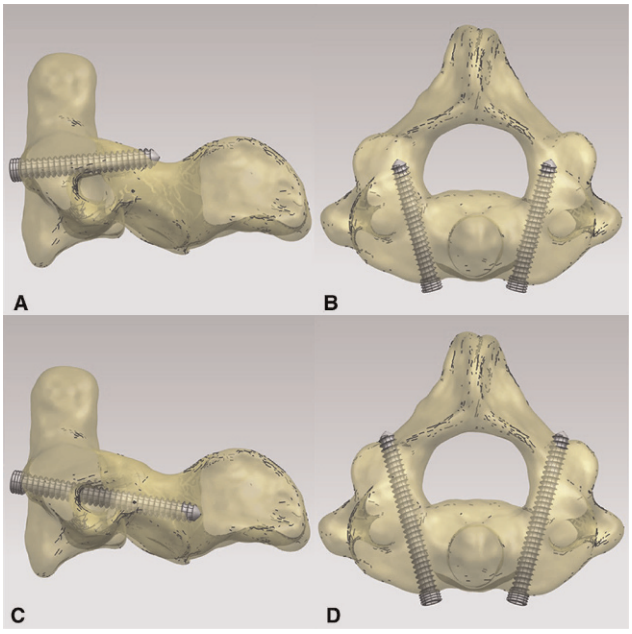

Figure 1 - A diagram showing the definitions of C2TOAMS and C2TOTPS. **A** The lateral view of C2TOAMS; **B** The axial view of C2TOAMS; **C** The lateral view of C2TOTPS; **D** The axial view of C2TOTPS.

counteract the redislocation strength between C1 and C2, we found that the medial and lateral cortical breach rate of C2TOAMS/C2TOTPS is high (46.9%, unpublished data), which can cause either concealed or manifest neurovascular injuries. We therefore developed the TARP-IV system and a set of individualized templates to assist transoral C2 screw placement and reduce potential neurovascular complications. We described and evaluated this system in this cadaveric study.

MATERIALS AND METHODS

With the approval of the institutional review board, ten fresh adult head-and-neck cadavers were obtained from the Department of Anatomy of Southern Medical University and kept at -20℃. After thawing, a transoral procedure was performed to expose the anterior surfaces of the C1 and C2 vertebrae and the articular tissues of the bilateral facet joints were completely resected. Then, the cranium was cut obliquely with a power saw from anterosuperior to posteroinferior and the brain tissue and spinal cord were then removed. A scalpel with a long handle was used to excise the transverse, alar and apical ligaments and other soft tissues around the odontoid through the transcranial approach, thereby creating simulated atlantoaxial dislocation between C1 and C2 (Figure 2).

A thin-sliced computed tomography (CT) scan was obtained from the cadavers and the data were obtained in DICOM format. The files were imported into Mimics software, version 10.0 (Materialise, Leuven, Belgium) and the C1 and C2 vertebrae were reconstructed in STL format. The STL files were imported into UG NX software, version 8.0 (Siemens PLM Software, Munich, Germany), in which simulative reduction was achieved and a TARP-IV of proper size was selected. Subsequently, a set of templates with cubic modules and drill guides were designed in UG NX

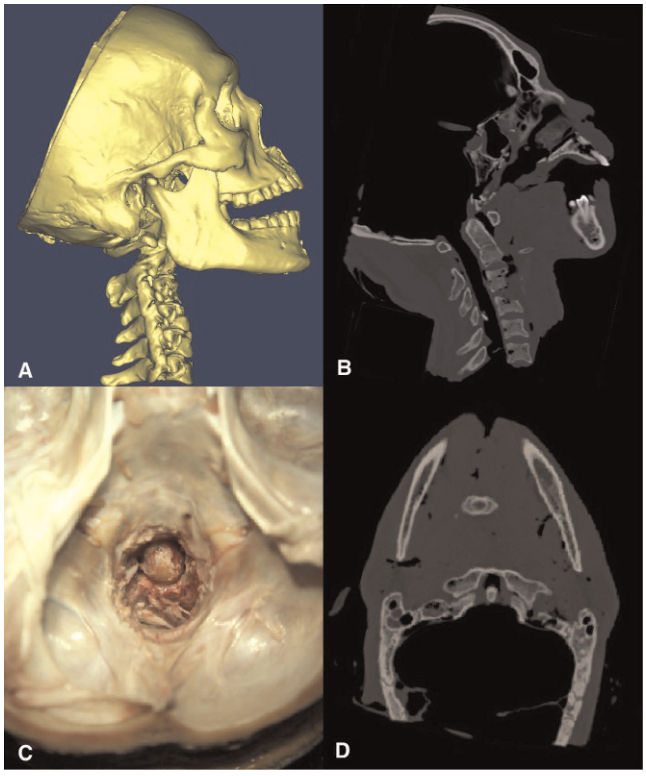

Figure 2 - A diagram showing the creation of simulative atlantoaxial dislocation. **A** Lateral view of the cadaver (CT reconstruction) after the creation of simulative dislocation; **B** Lateral-viewed CT scan; **C** Top view from the transcranial approach; **D** Axial-viewed CT scan.

8.0, according to the strategy shown in Figure 3. Three templates, A, B and C, were designed. A single template strategy could not be used due to the various relative positions among C1, C2 and the TARP-IV after atlantoaxial reduction. Template A served two purposes: it guided the drilling for the insertion of the reduction screw and it was used to drill a small hole for the placement of Template B at the center of the anterior surface of C2 later in the procedure. Template B was designed to assist the positioning of the TARP at the center of the anterior surface of C2. Furthermore, it assisted the vertical position measurement for the placement of the TARP by observing the level of the template that was aligned with the center of the plate hole for C2TOAMS/C2TOTPS placement after reduction. There were a total of 5 levels (the three convex bars and two concave ones between them, Figure 3F) and the central bar was the ideal level. The two adjacent concave bars were at levels 1 mm above and below the central bar and the two convex bars above and below these were located at levels 2 mm above and below. Template C was designed to guide the drilling for C2TOAMS/C2TOTPS insertion according to the measurement by Template B. Template C contained five drill guides corresponding to the five levels on Template B. Finally, the realistic templates were 3D printed using a stereolithography technique (Heng Tong company, China) (Figure 4).

The 10 cadavers were operated on in random order, two at a time. Two stages of experiments were performed, with 2 cadavers in stage one and 8 in stage two. In stage one, the drill sleeve was guided by a template with drill-sleeve-guiding

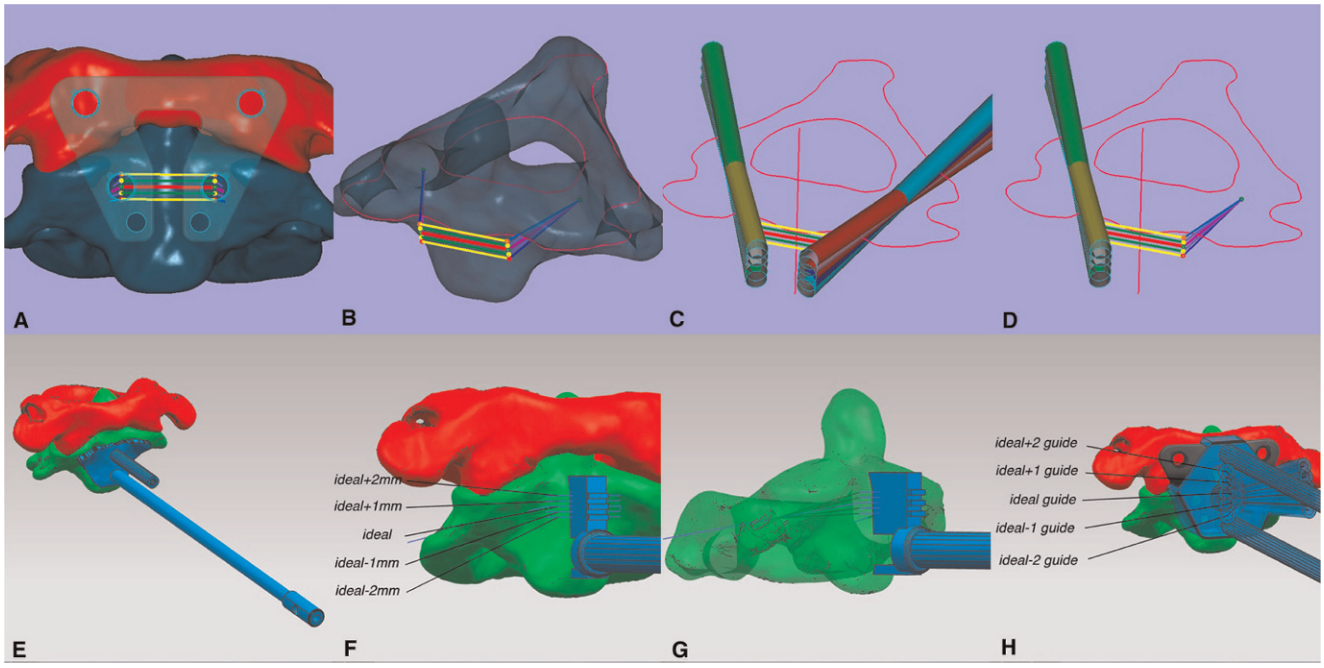

Figure 3 - A diagram showing the strategy of the template design. **A** Anterior view (the TARP-IV was situated at the ideal position). The green points: ideal screw entry points; the yellow points: 1 mm above or below the ideal screw entry points; the red points: 2 mm above or below the ideal screw entry points. **B** Anterolateral view. The two green points behind the possible screw entry points are the ideal screw passing points in the bilateral pedicles of C2. **C** and **D** The relationships between the possible screw trajectories and the contour of C2. **E** The positioning of Template A. **F** The positioning of Template B and the designing line graph (anterior view). **G** The positioning of Template B and the designing line graph (lateral view). **H** The positioning of Template C to the C1 and C2 anterior surfaces and the relationship between Template C and the TARP-IV.

channels (Figure 5A and B). During the procedure, we found that it was fairly difficult for the drill sleeve to be rotated into the polyaxial self-locking ring of the TARP-IV through the oblique guiding channels of Template C. Therefore, in stage two, the drill bit was guided by the template with drill guides (Figure 5C and D) and this procedure was performed on the remaining 8 cadavers. All of the cadaveric experiments were performed by the same surgeon without any fluoroscopic assistance.

After instrumentation, a CT scan was obtained from each cadaver and the data were imported into Mimics 10.0. The accuracy of C2TOAMS/C2TOTPS placement was graded according to the modified All India Institute of Medical Sciences outcome-based classification (6) as follows:

Type I: Ideal placement—screw threads are completely within the bony cortex;

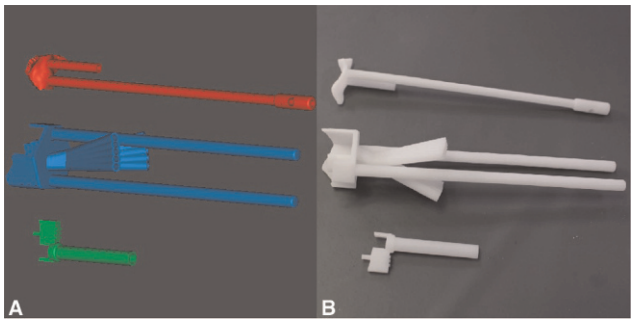

Figure 4 - A diagram showing the digital and realistic templates. **A** Digital 3D models of Templates A (red), B (green) and C (blue). **B** Realistic 3D models of the same templates.

Type II: Acceptable placement-less than 50% of the diameter of the screw violates the surrounding cortex; or

Type III: Unacceptable placement—clear violation of the transverse foramen or spinal canal.

In Mimics 10.0, the C2 vertebrae with C2TOAMS/C2TOTPS trajectories could be reconstructed in STL format. The STL files of C2 were imported into Geomagic Studio software, version 12.0 (Geomagic, USA) and the area around the C2TOAMS/C2TOTPS trajectories was selected and fit into two cylinders; then, these two cylinders and the postoperative C2 vertebra were exported together as one STL file. The planned screw trajectories of C2TOAMS/C2TOTPS were also fit into cylinders in UG NX 8.0 and then exported as one STL file, together with the preoperative C2 vertebra. The preoperative C2 with planned screw trajectories (cylinders) and the postoperative C2 with realistic screw trajectories (cylinders) were imported into Geomagic Studio 12.0. Subsequently, registration between the pre- and postoperative C2 vertebrae was performed. Finally, all of the aforementioned cylinders were transported to UG NX 8.0 in IGS format and the central line of these cylinders was determined to measure the distances between the planned and postoperative screw entry points on the frontal plane and the difference between the planned and postoperative screw angle orientation on the transverse and para-sagittal planes (Figure 6).

Statistical analysis was performed using a paired test to compare the distance and angle deviation between the planned and inserted screws.

Operative technique

The cadaver was placed in the supine position with the surgical field retracted by the CODMAN system. The

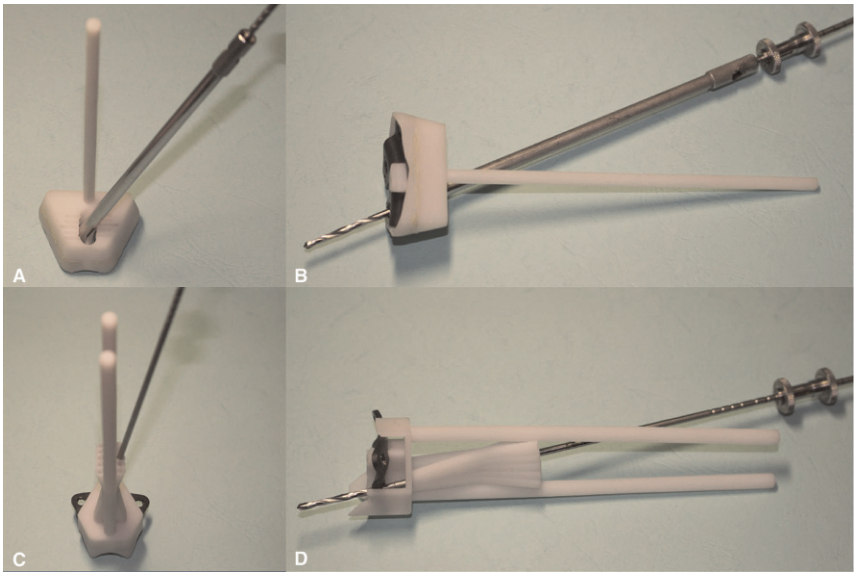

Figure 5 - A diagram showing the combination of Template C, the TARP-IV and the drill bit. **A** and **B** Template C adopted in stage one. **C** and **D** Template C adopted in stage two. Note the supralateral corners of Template C in stage two were removed in consideration of the shape of the wound.

anterior surfaces of C1 and C2 were exposed and the soft tissues were removed until the bony surface could be clearly observed. Template A was placed on the anterior surface of C2 until a lock-and-key configuration was achieved; then, a 2.5-mm drill bit was guided to drill the hole for the reduction screw. With the drill bit in position, another 2.5-mm drill bit was guided to drill the upper hole approximately 5 mm in depth for the placement of Template B. After the removal of Template A, a power drill was used to remove the anterior tubercle of C1 and a notch with a width of 10 mm was created at the inferior central border of the anterior arch of C1 for the placement of the reduction instrument. Subsequently, the anterior prominent edges of the bilateral C2 facets were flattened. After placement of the reduction screw, Template B, combined with the screwdriver, was placed at the anterior surface of C2, with its sleeve holding the screw head and its little pin inserted into the previously prepared upper bony hole. The TARP, held

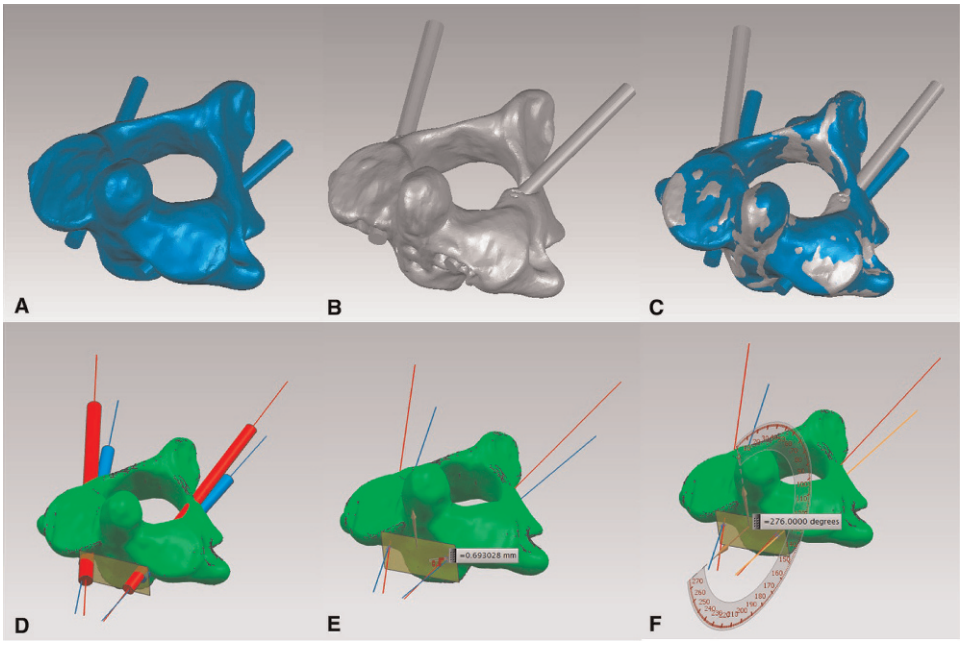

Figure 6 - A diagram showing the comparison between the planned and inserted screw trajectories. **A** The planned screw trajectories in C2. **B** The inserted screw trajectories in C2. **C** The registration between pre- and postoperative C2 vertebrae with screw trajectories. **D** The comparison between the planned and inserted screw trajectories and the configuration of the central lines of the screw trajectories. **E** The measurement of the deviations of the screw entry points. **F** The measurement of screw orientation on the parasagittal plane.

by the range finder, was then placed with the central slot engaging the cubic module of Template B and the upper two holes at the center of the anterior surface of the C1 lateral mass. A 1.5-mm K-wire was used to mark the entry point through the two canals within the two arms of the range finder. All of the devices were removed and then a gimlet was used to drill 10° laterally on the axial plane through the two marked entry points on the anterior surface of the C1 lateral mass. Then, the TARP was fastened to C1 with two C1ALMS so that the reduction screw would be in the center of the inferior slot of the TARP. After both arms of the reduction instrument had engaged the transverse beam of the TARP and the reduction screw, respectively, closure of the handgrips could impart local distraction force between C1 and C2. The longitudinal reduction process ended when the ''relative position'' of the inferior border of the TARP relative to the location of the reduction screw head was similar to that of the simulative reduction in UG NX 8.0 (Figure 7). Then, the nut on the upper arm of the reduction instrument was rotated to apply a posterior reduction force to the upper portion of the plate, displacing C1 posteriorly relative to C2. After reduction, two small unicortical holes were made by a hand drill through the two inferior holes of the TARP and two 2.0-mm locking screws were inserted. The reduction instrument was then removed. Template B was re-placed to measure the actual position of the two holes for C2TOAMS/C2TOTPS insertion (the ideal position or 1 mm/2 mm superior/inferior). Template B was removed and Template C was placed, engaging the plate and fitting onto the bony surface. With the five drill guides in Template C corresponding to the five levels of measurement on Template B, a 2.5-mm drill bit was used to drill through the corresponding drill guide of the template, according to the previous measurement by Template B. Then, the C2 vertebra was fixed relative to the reduced C1 vertebra by two C2TOAMS/C2TOTPS. The C2 reduction screw could now be removed and the midline wound was closed in two layers over the TARP (Figure 8).

RESULTS

Altogether, there were 20 C2TOAMS/C2TOTPS inserted into 10 cadavers, with 4 in stage one and 16 in stage two. In stage one, 2 C2TOAMS/C2TOTPS were graded as type I and the other 2 were graded as type III (Table 1). In stage two, 13 C2TOAMS/C2TOTPS were type I, 3 were type II and none were graded as type III. When the placement of the screws was compared with the planned placement, neither the distance between the entry points on both the x and y axes nor the difference in the transverse angles on the axial plane was statistically significant ($p>0.05$). However, the difference between the declination angles on the parasagittal plane was statistically significant ($p<0.05$) (Table 2).

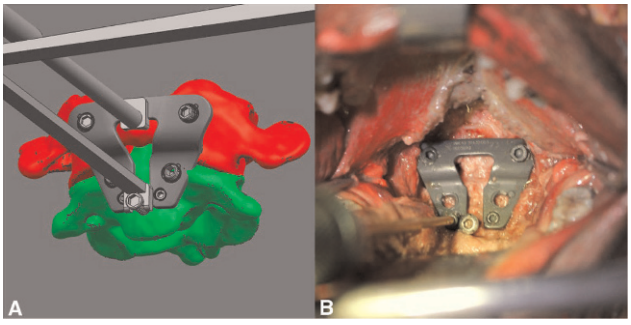

Figure 7 - A diagram showing the comparison between the digital and realistic final reduction positions. **A** The relationship between the reduction screw and the lower border of the TARP-IV in the planning phase. **B** The relationship between the reduction screw and the lower border of the TARP-IV in the cadaveric experiment. Note the lower border of the TARP-IV was aligned with the center of the reduction screw head in both diagrams.

DISCUSSION

In this study, we evaluated the use of the TARP-IV system in combination with a set of individualized templates to improve transoral C2 screw placement. Our findings suggested that simulation of the screw entry points and of the transverse angles of C2TOAMS/C2TOTPS could be achieved. However, the simulation of the declination angles of C2TOAMS/C2TOTPS was difficult due to the blockage of the drill bit and screwdriver by the upper teeth; in this situation, a planned ideal C2TOTPS would be placed as a C2TOAMS. However, with both the C2TOAMS and the C2TOTPS in the high bone density zone (7), there would not be any impact on the rigidness of fixation. There was already a drill sleeve in our TARP operative devices, which could be rotated into the polyaxial self-locking ring of the TARP to facilitate hand drill guidance. Therefore, in stage one, the TARP and drill sleeve complex were considered an integrated structure, which would be combined with Template C to guide screw placement. However, when an oblique channel was designed in the guiding template, it was fairly difficult for the drill sleeve to be rotated into the polyaxial self-locking ring through the channel after the close attachment between Template C and TARP-IV. As a result, the drill guides in Template C were designed to guide the hand drill directly, without using the drill sleeve in the second stage. This strategy proved to be effective so that the screw entry points and the transverse angles could be simulated. A realistic simulation of the transverse angles could be effective in reducing the possibility of medial or lateral cortex perforations of C2TOAMS/C2TOTPS, thus reducing the possibility of neurovascular injuries.

A variety of methods have been developed for accurate screw placement in the upper cervical area (8-27). Among them, anatomical landmarks and fluoroscopic device-assisted freehand screw placement are already used in daily practice. Other effective methods include navigation (20-23), drill guides made of stainless steel (17,23,28), robot assistance (18,24) and even assistance by microscope (27). There are mainly two problems impeding the application of navigation in transoral upper cervical procedures. First, the limited operative field and exposed bony surface make registration difficult. Second, the upper cervical structures are fairly mobile intraoperatively; thus, even when registration can be achieved, the ''migration phenomenon'' is inevitable. Robot-assisted accurate screw placement in the upper cervical area is still in its infancy, while microscope-assisted accurate screw placement has not been widely adopted. Drill guides made of stainless steel have also been reported by many authors (17,23,28), but for transoral upper cervical procedures, the space is too limited to manipulate these devices. Therefore, we decided to adopt the individualized-template strategy, as this strategy has been previously reported by many authors to assist posterior

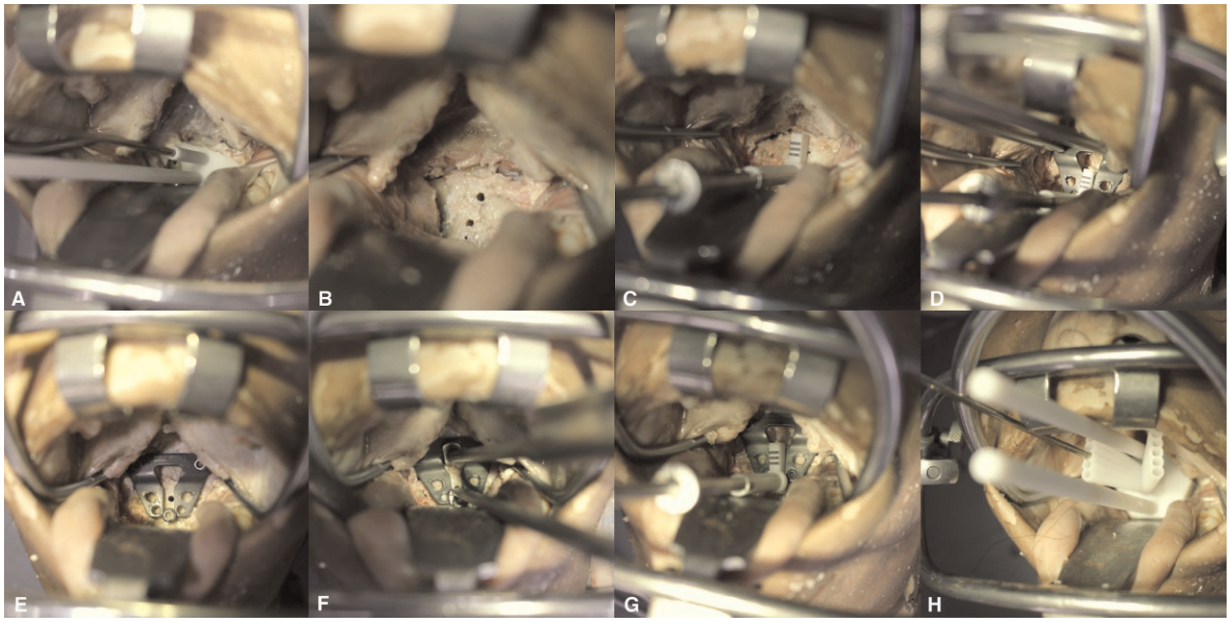

Figure 8 - A diagram showing the operative process with the templates. **A** The positioning of Template A on the C2 anterior surface and the bone drilling guided by it. **B** The drilled bone holes. **C** The positioning of Template B on the anterior surface of C2. **D** The positioning of the TARP-IV according to the location of the cubic module of Template B. **E** The relationship between the TARP-IV and the reduction screw head after it is fastened on C1. **F** Reduction process. **G** Measurement with Template B after the preliminary fixation of the TARP-IV on C2. **H** Template C-guided screw trajectory drilling. (The drilling was performed through the central ideal drill guide because the measurement showed that the centers of the screw holes in TARP-IV were aligned with the central ideal level of Template B in **Figure 8G**).

atlantoaxial screw placement (26,27,30,31). However, a grouped-template strategy has seldom been reported, mainly because systemic errors exist in the design and 3D-printing process of such templates; thus, the combination of templates means the combination of systemic errors. According to our limited experience, we felt that, using accurate 3D software and 3D-printing techniques, the systemic errors could be controlled and kept to a minimum level, which would be adequate to facilitate accurate upper cervical screw placement.

Many authors have reported the use of a posterior template to assist upper cervical screw placement and one advantage of using this strategy is the characteristic posterior atlantoaxial morphology (25,26,30). According to our observation, the anterior surface of C2 is also characteristic, with an anterior central prominence and two bilateral oblique grooves, making the use of a lock-and-key template possible. However, our TARP system serves both as a fixation and a reduction device. The entry points of C2TOAMS/C2TOTPS would be determined at the end of the reduction; therefore, designing a single lock-and-key template to assist screw placement would be impossible. During each TARP procedure, a reduction screw would be inserted as an anchor to counteract the reduction strength. In our strategy, we used the reduction screw as a reference for ''navigation''. Another anchoring site was the bony hole superior to the reduction screw, which we used to facilitate the firm positioning of Template B so that it could be placed at the center of the C2 anterior surface without swaying. The TARP would then be placed according to the cubic module of Template B and the possible entry points of C2TOAMS/C2TOTPS would then be symmetrically scattered bilaterally along the longitudinal axis of C2. During the design phase, the ideal reduction would be marked by the ''relative position'' between the reduction screw and the inferior border of the TARP and the intraoperative reduction would

Table 1 - Comparison of Planned *vs.* Inserted Screws (Stage I).

	Entry Point Differences		Angle Differences		
Cadaver	Dx	Dy	Transverse	Sagittal	Accuracy Evaluation
1R	0.18	-0.75	0.29	-15.26	I
1 L	3.45	-0.24	11.02	-5.76	III
2R	1.44	0.62	-0.63	-7.40	I
2 L	0.52	0.66	12.75	-3.85	III
M	1.40	0.07	5.86	-8.07	
S	1.47	0.69	7.01	5.01	

The first part of the table lists the differences (in millimeters) between the entry points of the planned and inserted screws ($D_{(x/y)} = D_{inserted}$-$D_{planned}$) on the coronal plane. The second part of the table lists the differences (in degrees) between the angles of the planned and inserted screws on the transverse and the para-sagittal planes. The x axis runs from left to right, and the y axis runs inferosuperior. L = left; R = right; m = mean; s = standard deviation; I = optimal; II = acceptable; III = unacceptable.

Table 2 - Comparison of Planned *vs.* Inserted Screws (Stage II).

	Entry Point Differences		Angle Differences		
Cadaver	Dx	Dy	Transverse	Sagittal	Accuracy Evaluation
3R	1.07	-0.83	3.79	-15.21	I
3 L	0.70	-0.84	-9.02	-18.26	II
4R	0.29	0.36	2.80	-8.81	I
4 L	1.15	0.75	-4.40	-12.23	I
5R	-0.56	-0.61	2.93	-1.56	I
5 L	-0.40	-0.67	1.11	-3.69	I
6R	0.34	-0.84	2.43	-9.60	I
6 L	0.54	-0.41	-1.09	-7.45	I
7R	0.71	0.91	0.82	-8.71	II
7 L	-0.43	0.96	-0.07	-13.68	I
8R	0.05	0.13	-2.51	-6.06	I
8 L	-0.28	-0.55	2.4	-15.02	II
9R	0.48	0.5	3.21	-12.65	I
9 L	-0.07	0.64	-2.49	-20.06	I
10R	-0.38	0.28	2.07	1.23	I
10 L	0.78	0.63	-1.36	-1.23	I
M	0.25	0.03	0.04	-9.56	
S	0.56	0.68	3.42	6.24	

The first part of the table lists the differences (in millimeters) between the entry points of the planned and inserted screws ($D_{(x/y)} = D_{inserted}-D_{planned}$) on the coronal plane. The second part of the table lists the differences (in degrees) between the angles of the planned and inserted screws on the transverse and the para-sagittal planes. The x axis runs from left to right and the y axis runs inferosuperior. L = left; R = right; m = mean; s = standard deviation; I = optimal; II = acceptable; III = unacceptable.

then simulate that ''relative position'', with which the deviation between the designed ideal entry points and the realistic entry points would not be more than 2 mm vertically, according to our experimental experience. Once the entry points of the C2TOAMS/C2TOTPS were determined by the simulation, the guided screw insertion would be accurate and safe.

There were some limitations to our study. First, the problem of ''blockage by the upper teeth'' could not be solved using this strategy, although it would not reduce the clinical effectiveness of this procedure. Second, the techniques for designing 3D models are relatively difficult for surgeons who are required to learn how to use 3D software. Third, because this was an exploratory study and cadavers are scarce, the sample size was small, which could have introduced bias to the design and experiments. Therefore, further studies with larger sample sizes should be performed before the procedure is used in clinical applications.

It is feasible to use individualized templates to guide transoral C2 screw placement. These drill templates combined with the TARP-IV system may improve the accuracy of transoral C2 screw placement and reduce related neurovascular complications.

■ ACKNOWLEDGMENTS

This study was supported by grants provided by the Science and Technology Project of Guangdong Province (2012B091000161 and 2012B031800187) and the Key Project of the Twelfth Five-year Project of Military Medicine (BWS11C065).

■ AUTHOR CONTRIBUTIONS

Li XS conceived and designed the study, was responsible for data acquisition analysis and interpretation, and manuscript drafting. Ai FZ, Xia H and Wu ZH were responsible for data analysis and interpretation, manuscript drafting, proofreading and revision as native English speakers. Ma XY, Zhang K, Wang JH, Mai XH study conceived and designed the study, and were responsible for the manuscript critical revision. Wu ZH and Yin QS conceived and designed the study, were responsible for the data analysis and interpretation and critical revision of the manuscript. Wu ZH and Yin QS contributed equally as co-corresponding authors.

■ REFERENCES

1. Wang C, Yan M, Zhou HT, Wang SL, Dang GT. Open reduction of irreducible atlantoaxial dislocation by transoral anterior atlantoaxial release and posterior internal fixation. Spine (Phila Pa 1976). 2006;31 (11):E306-13, http://dx.doi.org/10.1097/01.brs.0000217686.80327.e4",-1," xxx/80327.e4.
2. Visocchi M, Pietrini D, Tufo T, Fernandez E, Di Rocco C. Pre-operative irreducible C1-C2 dislocations: intra-operative reduction and posterior fixation. The ''always posterior strategy''. Acta Neurochir (Wien). 2009; 151(5):551-9, http://dx.doi.org/10.1007/s00701-009-0271-z.
3. Kandziora F, Pflugmacher R, Ludwig K, Duda G, Mittlmeier T, Haas NP. Biomechanical comparison of four anterior atlantoaxial plate systems. J Neurosurg. 2002;96(3 Suppl):313-20, http://dx.doi.org/10.3171/spi.2002.96.3.0313.
4. Yin Q, Ai F, Zhang K, Chang Y, Xia H, Wu Z, et al. Irreducible anterior atlantoaxial dislocation: one-stage treatment with a transoral atlantoaxial reduction plate fixation and fusion. Report of 5 cases and review of the literature. Spine (Phila Pa 1976). 2005;30(13):E375-81, http://dx.doi.org/10.1097/01.brs.0000168374.84757.d5.
5. Ai FZ, Yin QS, Xu DC, Xia H, Wu ZH, Mai XH. Transoral atlantoaxial reduction plate internal fixation with transoral transpedicular or articular mass screw of c2 for the treatment of irreducible atlantoaxial dislocation: two case reports. Spine (Phila Pa 1976). 2011;36(8):E556-62, http://dx.doi.org/10.1097/BRS.0b013e3181f57191.
6. Upendra BN, Meena D, Chowdhury B, Ahmad A, Jayaswal A. Outcome-based classification for assessment of thoracic pedicular screw placement. Spine (Phila Pa 1976). 2008;33(4):384-90, http://dx.doi.org/10.1097/BRS.0b013e3181646ba1.
7. Kandziora F, Schulze-Stahl N, Khodadadyan-Klostermann C, Schröder R, Mittlmeier T. Screw placement in transoral atlantoaxial plate systems: an anatomical study. J Neurosurg. 2001;95(1 Suppl):80-7, http://dx.doi.org/10.3171/spi.2001.95.1.0080.
8. Benzel EC. Anatomic consideration of C2 pedicle screw placement. Spine (Phila Pa 1976). 1996;21(19):2301-2, http://dx.doi.org/10.1097/00007632-199610010-00028.
9. Jun BY. Anatomic study for ideal and safe posterior C1-C2 transarticular screw fixation. Spine (Phila Pa 1976). 1998;23(15):1703-7, http://dx.doi.org/10.1097/00007632-199808010-00018.
10. Resnick DK, Lapsiwala S, Trost GR. Anatomic suitability of the C1-C2 complex for pedicle screw fixation. Spine (Phila Pa 1976). 2002;27(14): 1494-8, http://dx.doi.org/10.1097/00007632-200207150-00003.
11. Simsek S, Yigitkanli K, Seckin H, Akyol C, Belen D, Bavbek M. Freehand C1 lateral mass screw fixation technique: our experience. Surg Neurol. 2009;72(6):676-81, http://dx.doi.org/10.1016/j.surneu.2009.06.015.

12. Chun HJ, Bak KH. Targeting a safe entry point for c2 pedicle screw fixation in patients with atlantoaxial instability. J Korean Neurosurg Soc. 2011;49(6):351-4, http://dx.doi.org/10.3340/jkns.2011.49.6.351.
13. Ondra SL, Marzouk S, Ganju A, Morrison T, Koski T. Safety and efficacy of C2 pedicle screws placed with anatomic and lateral C-arm guidance. Spine (Phila Pa 1976). 2006;31(9):E263-7, http://dx.doi.org/10.1097/01.brs.0000214882.34674.be.
14. Yeom JS, Buchowski JM, Park KW, Chang BS, Lee CK, Riew KD. Lateral fluoroscopic guide to prevent occipitocervical and atlantoaxial joint violation during C1 lateral mass screw placement. Spine J. 2009;9(7):574-9.
15. Tessitore E, Bartoli A, Schaller K, Payer M. Accuracy of freehand fluoroscopy-guided placement of C1 lateral mass and C2 isthmic screws in atlanto-axial instability. Acta Neurochir (Wien). 2011;153(7):1417-25, http://dx.doi.org/10.1007/s00701-011-1039-9.
16. Weidner A, Wähler M, Chiu ST, Ullrich CG. Modification of C1-C2 transarticular screw fixation by image-guided surgery. Spine (Phila Pa 1976). 2000;25(20):2668-74, http://dx.doi.org/10.1097/00007632-200010150-00020.
17. Gebhard JS, Schimmer RC, Jeanneret B. Safety and accuracy of transarticular screw fixation C1-C2 using an aiming device. An anatomic study. Spine (Phila Pa 1976). 1998;23(20):2185-9, http://dx.doi.org/10.1097/00007632-199810150-00008.
18. Lee JY, Lega B, Bhowmick D, Newman JG, O'Malley BW Jr, Weinstein GS, et al. Da Vinci Robot-assisted transoral odontoidectomy for basilar invagination. ORL J Otorhinolaryngol Relat Spec. 2010;72(2):91-5, http://dx.doi.org/10.1159/000278256.
19. Welch WC, Subach BR, Pollack IF, Jacobs GB. Frameless stereotactic guidance for surgery of the upper cervical spine. Neurosurgery. 1997;40(5):958-64, http://dx.doi.org/10.1097/00006123-199705000-00016.
20. Hurlbert RJ. Frameless stereotactic guidance for surgery of the upper cervical spine. Neurosurgery. 1997;41(6):1448-9, http://dx.doi.org/10.1097/00006123-199712000-00054.
21. Tian W, Weng C, Li Q, Liu B, Sun YQ, Yuan Q, et al. Occipital-C2 transarticular fixation for occipitocervical instability associated with occipitalization of the atlas in patients with klippel-feil syndrome, using intraoperative 3-dimensional navigation system. Spine (Phila Pa 1976). 2013;38(8):642-9, http://dx.doi.org/10.1097/BRS.0b013e31827a330a.
22. Börm W, König RW, Albrecht A, Richter HP, Kast E. Percutaneous transarticular atlantoaxial screw fixation using a cannulated screw system and image guidance. Minim Invasive Neurosurg. 2004;47(2):111-4, http://dx.doi.org/10.1055/s-2004-818449.
23. Ito Y, Hasegawa Y, Toda K, Tanaka M, Nakahara S. The original hole-in-one guide for atlantoaxial transarticular screw fixation. J Orthop Sci. 2001;6(1):16-21, http://dx.doi.org/10.1007/s007760170019.
24. Kostrzewski S, Duff JM, Baur C, Olszewski M. Robotic system for cervical spine surgery. Int J Med Robot. 2012;8(2):184-90.
25. Goffin J, Van Brussel K, Martens K, Vander Sloten J, Van Audekercke R, Smet MH. Three-dimensional computed tomography-based, personalized drill guide for posterior cervical stabilization at C1-C2. Spine (Phila Pa 1976). 2001;26(12):1343-7, http://dx.doi.org/10.1097/00007632-200106150-00017.
26. Lu S, Xu YQ, Lu WW, Ni GX, Li YB, Shi JH, et al. A novel patient-specific navigational template for cervical pedicle screw placement. Spine (Phila Pa 1976). 2009;34(26):E959-66, http://dx.doi.org/10.1097/BRS.0b013e3181c09985.
27. Liu G, Buchowski JM, Shen H, Yeom JS, Riew KD. The feasibility of microscope-assisted ''free-hand'' C1 lateral mass screw insertion without fluoroscopy. Spine (Phila Pa 1976). 2008;33(9):1042-9, http://dx.doi.org/10.1097/BRS.0b013e31816d72b5.
28. Neo M, Matsushita M, Yasuda T, Sakamoto T, Nakamura T. Use of an aiming device in posterior atlantoaxial transarticular screw fixation. Technical note. J Neurosurg. 2002;97(1 Suppl):123-7.
29. Ryken TC, Owen BD, Christensen GE, Reinhardt JM. Image-based drill templates for cervical pedicle screw placement. J Neurosurg Spine. 2009;10(1):21-6, http://dx.doi.org/10.3171/2008.9.SPI08229.
30. Kawaguchi Y, Nakano M, Yasuda T, Seki S, Hori T, Kimura T. Development of a new technique for pedicle screw and Magerl screw insertion using a 3-dimensional image guide. Spine (Phila Pa 1976). 2012;37(23):1983-8, http://dx.doi.org/10.1097/BRS.0b013e31825ab547.